Article

Bi-Symmetric Polyhedral Cages with Maximally Connected Faces and Small Holes

Bernard Piette * and **Árpad Lukács**

Department of Mathematical Sciences, Durham University, Durham DH1 3LE, UK; lukacs.arpad@gmail.com
* Correspondence: b.m.a.g.piette@durham.ac.uk

Abstract: Polyhedral cages (p-cages) describe the geometry of some families of artificial protein cages. We identify the p-cages made out of families of equivalent polygonal faces such that the faces of one family have five neighbors and P_1 edges, while those of the other family have six neighbors and P_2 edges. We restrict ourselves to polyhedral cages where the holes are adjacent to four faces at most. We characterize all p-cages with a deformation of the faces, compared to regular polygons, not exceeding 10%.

1. Introduction

A few years ago, J. Heddle created an artificial protein cage made out of 24 so-called rings, which were themselves made out of 11 copies of the same protein called TRAP [1]. The nano-cage appears to be a regular structure made out of 24 hendecagons, with some small holes, which is mathematically impossible. It was shown that the faces of the corresponding structure are not regular but that the deformations of their edge lengths and angles, compared to those of the corresponding regular polygon, are less than half a percent [2], making them look regular to the naked eye. These small deformations can easily be absorbed by the proteins and the termini where the faces are linked together. A small nano-cage made out of the same ring but counting only 12 of them was made in the same lab [3]. This was also identified as a nearly regular structure but one where the deformations are approximately 2.5%.

These discoveries led us to define polyhedral cages [4] (p-cages for short) as assemblies of polygons with holes, requiring that each face shares edges with at least three other faces and also imposing that of any two adjacent edges of a face, only one can be shared. While the faces must be planar convex polygons, the holes can have any shape. In what follows, we only consider convex p-cages, as defined in [4,5].

P-cages are said to be regular if all the faces are regular and near-miss if they are slightly deformed. Homogeneous p-cages are made out of polygons with the same number of edges, while bi-homogeneous p-cages are made out of two types of polygons. In [5], we defined symmetric p-cages as p-cages for which any two faces can be mapped into each other via a rotation that is an automorphism of the p-cage. Similarly, bi-symmetric p-cages are bi-homogeneous p-cages for which any two faces belonging to the same family can be mapped into each other via a rotation automorphism of the p-cage [6].

When we consider near-miss p-cages, we must decide how large a deformation, defined formally later, we are willing to consider. In [4,5], we have identified all regular and near-miss symmetric p-cages made out of polygons with up to 20 edges and with

deformations not exceeding 10%. In [6], we have identified the bi-symmetric p-cages where each face of a given type only shares edges with faces of the other type, again restricting ourselves to 10% of deformation and polygons with up to 20 edges.

The aim of this paper is to identify bi-symmetric p-cages where the faces have a maximum number of neighbors. As it is not possible for all the faces to have six neighbors [7], we consider p-cages for which the faces of the first type have five neighbors each while the faces of the second type have six.

So far, a number of artificial protein cages have been experimentally generated [8–13]. The main aim is to develop new drug delivery methods [14–18]. The idea is to encapsulate the drug inside the cage while specific receptors are linked to the holes outside the cage to bind with the cells that are targeted, such as cancer cells [14]. Once absorbed by the cell, the protein cage can release the drug in the cytoplasm [19]. This will lead to more efficient drug delivery, as a smaller amount of the drug must be provided, with the bonus of reduced side effects, as only the targeted cells will be affected.

While the virus capsids found in nature are essentially based on the geometry of platonic solids [20], some of the cages created experimentally exhibit somewhat different structures [2,3,21]. It is then natural to ask the question as to what geometries are possible for such cages [22–24].

One of the ultimate aims of nano–bio engineers is to use these artificial protein cages to perform targeted drug delivery. The aim of this paper is to find further potential geometries for nano-protein cages, identifying all bi-symmetric ones with maximal connectivity between the faces as well exhibiting small holes. Nano–bio engineers design artificial protein cages using protein assemblies forming, approximately, regular polygons. These experiments are expensive and time consuming, so our aim is to identify geometries that can be achieved, identifying the polygons most likely to lead to cages of a given size. As the suitable geometries achievable with a single type of polygon are limited in number and in size [4,5], in this paper we consider some cages made out of two types of protein faces to suggest to the experimentalists which polygons to use and combine. To validate our approach, we should also point out that the geometries obtained in [4,5] predicted the geometries obtained by the Heddle lab with their 12-gon protein rings in [25].

2. Methodology

As described in [4], to construct a p-cage, one must first consider the planar graph obtained by joining the centers of the neighboring faces of the p-cage with straight lines. We call the resulting object the hole polyhedron graph, as its faces describe how many faces surround each hole. The nodes of the hole polyhedron graph correspond to the faces of the p-cage, while the edges describe how the faces are joined together.

Our aim in this paper is to construct p-cages made out of two families of faces such that each face of a given family can be mapped by an automorphism rotation of the p-cage to any other face of the same family.

In what follows, we define as the valency of a face the number of neighbors that it has. As we are interested in p-cages with the maximum number of neighbors, we impose that the faces belonging to the first family has a valency of 5 while the other faces have a valency of 6. As we are interested only in p-cages with small holes, we also impose that the faces of the hole polyhedron graphs are triangles, squares, or any mix of each.

There are only nine such graphs [7] as listed in Table 1.

The naming convention of the graphs is described in [7], but the end of these names is particularly useful, as in Vn_m, n and m correspond respectively to the numbers of pentavalent and hexavalent nodes and hence also correspond to the numbers of p-cage faces with five and six neighbors, respectively.

Table 1. Bi-symmetric hole polyhedron graphs with valency 5 and 6 nodes as well as triangular and square faces [7]. The first column is the label we use to describe the p-cages derived from the graph, the second column is the label for the graph used in [7], and the third column describe a solid for which the planar graph corresponds to the hole polyhedron graph. N-mosaic were defined in [7] as 2N-gons with an extra edge attached to every other node.

p-Cage Name	Graph Name	Description
HAP6	56_F24_12-2-1_12-3-0_V12_2	Hexagonal anti-prism with a hexagonal pyramid on each base.
TTP6	56_F28_4-3-0_24-2-1_V12_4	Truncated tetrahedron where a pyramid is placed on each hexagon.
TTM3	56_F44_4-0-3_4-3-0_12-2-1_24-1-2_V12_12	Truncated tetrahedron where the hexagons become 3-mosaic.
TOP6	56_F54_6-4-0_48-2-1_V24_8	Truncated octahedron where a pyramid is placed on the hexagons.
PD	56_F60_60-1-2_V12_20	Pentakis dodecahedron.
IP5	56_F80_20-0-3_60-1-2_V12_30	Pyramids on the faces of an icosidodecahedron.
TOM3	56_F86_6-0-4_8-3-0_24-2-1_48-1-2_V24_24	Truncated octahedron where the hexagons are 3-mosaic.
TCM4	56_F86_6-4-0_8-0-3_24-2-1_48-1-2_V24_24	Truncated cube where the octagons are 4-mosaic.
SDP5	56_F140_60-1-2_80-0-3_V12_60	Pyramids on the faces of a snub dodecahedron.

In what follows, we denote by P_1 and P_2 the numbers of edges of the faces belonging to families 1 and 2, respectively. When a polygon with P edges has n neighbors, its has $P - n$ edges that must be distributed between the n edges adjacent to neighbor faces. If we use the labels `a`, `b`, `c`, `d`, and `e`, to label the numbers of edges given to each hole by the first family of faces and `A`, `B`, `C`, `D`, `E`, and `F` for the second family, we have the following:

$$\texttt{a + b + c + d + e} + 5 = P_1, \quad \texttt{A + B + C + D + E + F} + 6 = P_2 \tag{1}$$

for the faces belonging respectively to the first and the second families. We must then find out how to distribute them on each of the identified hole polyhedron graphs in such a way that the equivalence between the faces is preserved. We now consider each of these nine graphs one by one:

For `HAP6`, the corners of the valency 6 nodes must all be identical, but the corners around the valency 5 nodes can be arbitrary (Figure 1a).

For `TTP6`, the corners of the valency 6 nodes must be alternating `A-B-A-B-A-B`, but then the corners of the valency 5 nodes can be arbitrary (Figure 1b).

For `TOP6`, the corners of the valency 5 nodes are arbitrary and mapped as in Figure 2a. The corners of the valency 6 nodes must then alternate between `A` and `B` (Figure 2a).

For `PD`, the equivalence between two adjacent valency 6 nodes is achieved either via a five-fold rotation around the pyramid or via a 2π rotation around the center of the link joining them. In either case, we see that the corners around the valency 5 nodes must all be equal. Then the corners of the valency 6 nodes must be alternatingly `A` and `B` (Figure 2b).

For `IP5`, we see that by symmetry, the corners of the triangles joining the valency 6 nodes must all be the same so the corners of the valency 5 nodes are also all identical. Then, for the valency 6 nodes, we have the sequence `A-B-C-A-B-C` (Figure 3a).
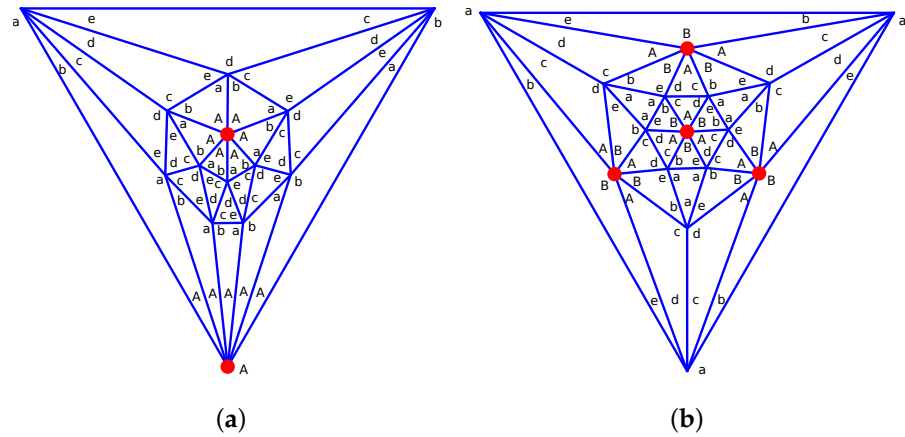
Figure 1. Hole-edges mapping for the hole polyhedron graphs: (**a**) HAP6; (**b**) TTP6. The red dots are the hexavalent nodes. See the main text for the definition of the corner labels.
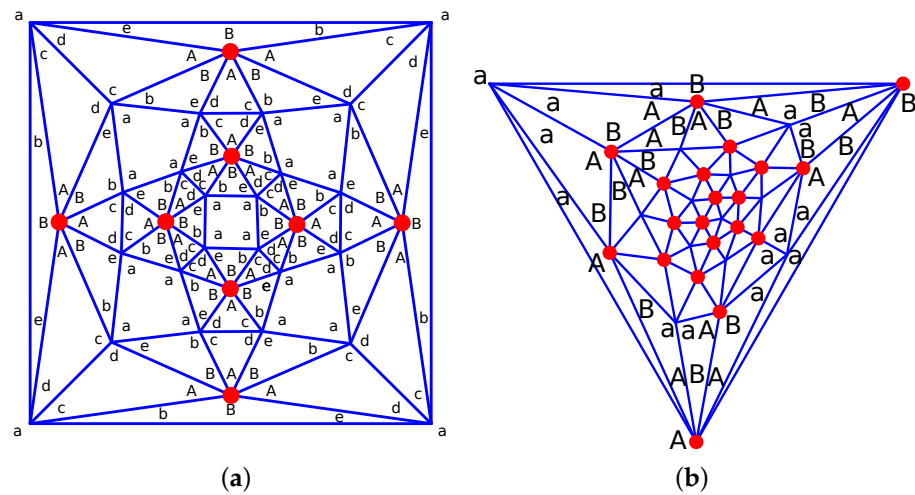
Figure 2. Hole-edges mapping for the hole polyhedron graphs: (**a**) TOP6; (**b**) PD. The red dots are the hexavalent nodes. See the main text for the definition of the corner labels.
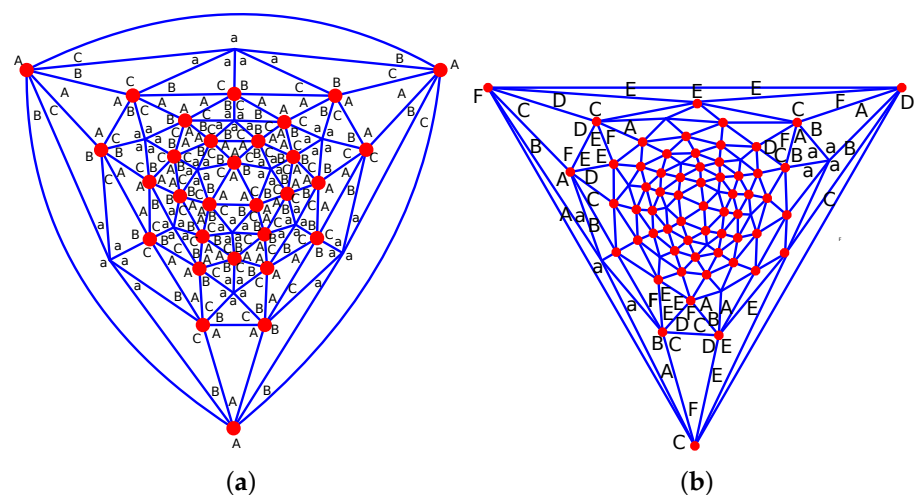
Figure 3. Hole-edges mapping for the hole polyhedron graphs: (**a**) IP5; (**b**) SDP5. The red dots are the hexavalent nodes. See the main text for the definition of the corner labels.

For SDP50, the corners around the valency 5 nodes must all be the same, but then the corners around the valency 6 nodes are arbitrary, as shown in the figure (Figure 3b).

The p-cages `TTM3` and `TOM3` do not lead to any valid p-cages with deformations below 10% and the best `TCM3` p-cages having deformations exceeding 8% are not good candidates for protein cages, as the faces are too irregular for protein rings to adjust to the deformations. For this reason, the construction of these three families of cages is described in the Supplementary Materials.

To construct the p-cages, we follow a method similar to the one described in [5,6]: we derive the most general parametrization for the different faces, which we then use to numerically determine the faces that are the least irregular.

First, we notice that each of the identified hole polyhedron graphs are built from an Archimedean solid, the dual of an Archimedean solid, or an anti-prism. Given a face of any of the two families, all of the other faces of the same family will be obtained by applying the symmetry of the regular solid underlying the hole polyhedron graph. We label each face with its family type j, set to 1 for the pentavalent faces and 2 for the hexavalent faces, and an index number i. Each face will belong to a plane going through the vector $V_{j,i}$ and spanned by the orthonormal basis vectors $v_{j,i,1}$ and $v_{j,i,2}$. We also chose $V_{j,i}$ such that it is orthogonal to the considered plane. The planes and faces with index $i = 1$ are called the reference plane and face, respectively. The remaining faces of the p-cage can then be obtained by applying a rotation to the reference faces. We can then determine the lines of intersection between adjacent faces, knowing that the shared edges will lie on these lines. The vertices of the reference faces can then be parametrized in the reference plane, restricting the vertices belonging to two faces to lie on the corresponding intersection lines. The vertices belonging to a hole will belong to the reference plane without any further restriction.

We then have to identify the face configuration for which the faces are as regular as possible.

First, we denote n_i, $i = 0, P_{j-1}$ as the vertices of a face, ordered anti-clockwise when seen from outside the p-cage, and m_{f_j} as the normal to the reference face of type j pointing out of the p-cage. We then define the edge vector $s_i = n_i - n_{(i+1) \bmod P_j}$ so that the edge lengths are given by $d_i = |s_i|$ and compute the angle α_i between adjacent edges, by evaluating $s_i \times s_{i+1}$ and

$$
\begin{aligned}
\text{if } (s_i \times s_{i+1}) \cdot m_{f_j} \geq 0 \quad &: \quad \alpha_i = \pi - \arccos\left(\frac{(s_i \cdot s_{i+1})}{|s_i||s_{i+1}|}\right), \\
\text{if } (s_i \times s_{i+1}) \cdot m_{f_j} < 0 \quad &: \quad \alpha_i = \pi + \arccos\left(\frac{(s_i \cdot s_{i+1})}{|s_i||s_{i+1}|}\right).
\end{aligned}
\tag{2}
$$

Note, that α_i in (2) corresponds to the angle inside the face, which is larger than π if the face is not convex. For a regular P-polygon, $\alpha = \pi(1 - \frac{2}{P})$.

After computing the d_i and α_i, we can minimize the deviation from the regularity energy as follows:

$$
E = \frac{1}{P_1 + P_2} \left(E_1 + E_2 + c_c\, E_{\text{Fconv}} + c_{pc}\, E_{\text{Pconv}} \right)
\tag{3}
$$

where:

$$
E_j = \sum_{i=0}^{P_j-1} \left[c_l \left(\frac{d_i - L}{L} \right)^2 + c_a \left(\frac{\alpha_i - \pi(1 - \frac{2}{P_j})}{\pi(1 - \frac{2}{P_j})} \right)^2 \right], \quad j = 1, 2
\tag{4}
$$

with the three weight factors c_l, c_a, and c_c. In (4), the first term measures the deviation of the edge lengths d_i from the target length L, while the second term measures the deviation of the inside angles, α_i, between adjacent face edges from the corresponding angles of the regular P-gon. E_{Fconv} is given explicitly by the following:

$$E_{\text{Fconv}} = \sum_{j=1,2} \frac{1}{P_j} \sum_i \left[H\left(-(s_i \times s_{i+1}) \cdot m_{f_j} \right) \right] \tag{5}$$

where $H(x)$ is the Heaviside function. Equation (5) results in 0 unless the polygon defined by the vertices is concave.

To compute E_{Pconv}, we find C_i, the position of the center of face i, if we consider the two adjacent faces C_i and C_j with the normal vectors m_i and m_j, respectively. The p-cage is convex if for all pairs of adjacent faces, the distance between the centers of the two faces is smaller than the distance between $C_i + m_i$ and $C_j + m_j$. This is used to define E_{Pconv} as follows:

$$E_{\text{Pconv}} = \sum_{j=1,2} \left[\frac{1}{P_j} \sum_{i \in I_j} \left[H\left(|C_i - C_j|^2 - |C_i + m_i - C_j - m_j|^2 \right) \right] \right]. \tag{6}$$

where I_j is the set of faces, of any type, adjacent to the reference face j. Note, that E_{Pconv} is 0 unless the p-cage is concave.

To ensure the convexity of bi-symmetric p-cages and minimize the irregularity in their geometric parameters, we use a simulated annealing algorithm [26], which varies the parameters of the p-cages to minimize E and hence find the optimal configuration for each p-cage.

In particular, the last two terms, E_{Pconv} and E_{Fconv}, are used in the simulated annealing optimization procedure to enforce the convexity of the faces and the p-cage by taking large values for c_c and c_{pc}. In (3), we divide the sum by $P_1 + P_2$ to make the parametrization of the optimizing algorithm easier.

To characterize the deviation from the regularity of a p-cage we define the deformation of its edge length and angles as follows:

- Length: $\Delta_l = \max_i \left(\left| \frac{d_i - L}{L} \right| \right)$
- Angle: $\Delta_l = \max_i \left(\left| \frac{\alpha_i - \pi(1 - \frac{2}{p})}{\pi(1 - \frac{2}{p})} \right| \right)$

3. Notation

In what follows we denote with $R_w(\theta)$ as a rotation of the angle θ around the vector w. We also denote $R_x(\theta)$, $R_y(\theta)$, and $R_z(\theta)$ as the rotation of an angle θ around the respective axes x, y, and z.

The plane of face j, i can be parametrized using the point $V_{j,i}$ contained in the plane and the plane basis vectors $v_{j,i,1}$ and $v_{j,i,2}$ as follows:

$$\mathcal{P}_{j,i}(t_1, t_2) = V_{j,i} + t_1 v_{j,i,1} + t_2 v_{j,i,2}. \tag{7}$$

Given two such planes with parametrizations $\mathcal{P}_{j_1,i}$ and $\mathcal{P}_{j_2,k}$, we must find the intersecting line, which determines where the edge shared by the two adjacent faces is. First, we define the normal vectors to each planes, $p_{j_1,i}$ and $p_{j_1,k}$, as well as the vector $u_{j_1,i;j_2k}$ parallel to the plane intersection:

$$p_{j_1,i} = v_{i,1} \times v_{i,2}, \qquad p_{j_2,k} = v_{j,1} \times v_{j,2}, \qquad u_{j_1,i;j_2,k} = p_{j_1,i} \times p_{j_2,k}. \tag{8}$$

Any point $U_{j1,i1,j2,i2}$ on that line is in the range of the parametrizations of both planes:

$$U_{j_1,i;j_2,k} = V_{j_1,i} + t_1 v_{j_1,i,1} + t_2 v_{j_1,i,2} = V_{j_2,k} + s_1 v_{j_2,k,1} + s_2 v_{j_2,k,2}. \tag{9}$$

If that point is perpendicular to $u_{j1,i1,j2,i2}$, then a relation holds among t_1, t_2 and s_1, s_2, obtained by multiplying both sides of (9) by $u_{j_1,i;j_2,k}$, which, as detailed in [5], when inserted back into (9), gives the following:

$$
U_{j_1,i;j_2,k} = V_{j_1,i} + \frac{(p_{j_2,k} \cdot (V_{j_2,k} - V_{j_1,i}))(u_{j_1,i;j_2,k} \cdot v_{j_1,i,2}) + (u_{j_1,i;j_2,k} \cdot V_{j_1,i})(p_{j_2,k} \cdot v_{j_1,i,2})}{(p_{j_2,k} \cdot v_{j_1,i,1})(u_{j_1,i;j_2,k} \cdot v_{j_1,i,2}) - (u_{j_1,i;j_2,k} \cdot v_{j_1,i,1})(p_{j_2,k} \cdot v_{j_1,i,2})} \times
$$
$$
\left(v_{j_1,i,1} - \frac{(u_{j_1,i;j_2,k} \cdot v_{j_1,i,1})}{(u_{j_1,i;j_2,k} \cdot v_{j_1,i,2})} v_{j_1,i,2} \right) - \frac{(u_{j_1,i;j_2,k} \cdot V_{j_1,i})}{(u_{j_1,i;j_2,k} \cdot v_{j_1,i,2})} v_{j_1,i,2}. \tag{10}
$$

To obtain the intersection point of two coplanar lines, $U_{j_1,i} + \lambda u_{j_1,i}$ and $U_{j_2,k} + \mu u_{j_2,k}$, where we assume $u_{j_1,i}$ and $u_{j_2,k}$ to be normalized to 1, we need to find the value of λ so that

$$
U_{j_1,i} + \lambda u_{j_1,i} = U_{j_2,k} + \mu u_{j_2,k} \tag{11}
$$

Multiplying (11) by respectively $u_{j_1,i}$ and $u_{j_2,k}$ we obtain the following:

$$
\lambda = (U_{j_2,k} - U_{j_1,i})u_{j_1,i} + \mu(u_{j_2,k} \cdot u_{j_1,i})
$$
$$
\mu = (U_{j_1,i} - U_{j_2,k})u_{j_2,k} + \lambda(u_{j_1,i} \cdot u_{j_2,k}). \tag{12}
$$

Substituting the second equation into the first one, we obtain the following for the point of intersection:

$$
P_{j_1,i;j_2,k} = U_{j_1,i} + u_{j_1,i} \left(\frac{((U_{j_2,k} - U_{j_1,i}) \cdot (u_{j_1,i} - u_{j_2,k}(u_{j_1,i} \cdot u_{j_2,k})))}{1 - (u_{j_1,i} \cdot u_{j_2,k})^2} \right). \tag{13}
$$

In what follows, $P_{j_1,i;j_2,k}$ will denote the intersection point between the following three faces: the reference face of type 1, the face i of type j_i, and the face k, of type j_2. This corresponds to the intersection point between the two lines $U_{1,1;j_1,i} + \lambda u_{1,1;pj_1,i}$ and $U_{1,1;j_2,k} + \lambda u_{1,1;j_2,k}$ obtained using (13). Similarly, $Q_{j_1,i;j_2,k}$ will denote the intersection point between the reference face of type 2, the face i of type j_i, and the face k of type j_2.

To denote face i of type j, we use the notation $F_{j,i}$, and each face with index $i > 1$ is related to the references face of the correct type via a rotation:

$$
F_{1,i} = \mathcal{R}_{1,i} F_{1,1}, \quad F_{2,i} = \mathcal{R}_{2,i} F_{2,1}. \tag{14}
$$

The spanning vectors $V_{j,i}$, $v_{j,i,1}$, and $v_{j,i,1}$ will then be obtained via the same rotation:

$$
Vj,i = \mathcal{R}_{j,i} V_{j,1}, \quad vj,i,1 = \mathcal{R}_{j,i} v_{j,1,1}, \quad vj,i,1 = \mathcal{R}_{j,i} v_{j,1,1}. \tag{15}
$$

4. Parametrization

4.1. HAP6

The symmetry of the `HAP6` p-cage is that of the hexagonal anti-prism. For the reference face vectors, we chose the following:

$$V_{1,1} = S_1 (0, \cos(\theta_2), -\sin(\theta_2))^t, \qquad V_{2,1} = S_2 (0,0,1)^t \tag{16}$$
$$v_{1,1,1} = (1,0,0), \qquad v_{1,1,2} = (0, \sin(\theta_2), \cos(\theta_2)) \tag{17}$$
$$v_{2,1,1} = (1,0,0), \qquad v_{2,1,2} = (0,1,0). \tag{18}$$

and the rotations between the faces are:

$$\mathcal{R}_{1,i} = R_z\left(\frac{i\pi}{3}\right), \quad i = 2\ldots 6 \qquad \mathcal{R}_{1,i} = R_z\left(\frac{(1+2i)\pi}{6} + \sigma\right)R_y(\pi), \quad 1 = 7\ldots 12 \quad (19)$$

$$\mathcal{R}_{2,2} = R_z\left(\frac{\pi + \sigma}{6}\right)\right)R_y(\pi) \tag{20}$$

where σ is an angle that allows the top and bottom halves of the p-cages to be shifted sideways with respect to each other.

The nodes of the reference face of type 1 shared with the adjacent faces are (Figure 4a,b).

$$\boldsymbol{n}_1 = P_{1,2;1,7} + k_1\boldsymbol{u}_{1,1;1,2}, \qquad\qquad \boldsymbol{n}_2 = P_{1,2;1,7} + k_2\boldsymbol{u}_{1,1;1,2}, \tag{21}$$

$$\boldsymbol{n}_3 = P_{1,2;2,1} + k_3\boldsymbol{u}_{2,1;1,1}, \qquad\qquad \boldsymbol{n}_4 = P_{1,2;2,1} + k_4\boldsymbol{u}_{2,1;1,1}, \tag{22}$$

$$\boldsymbol{n}_5 = R_z\left(\frac{-\pi}{3}\right)\boldsymbol{n}_2 \qquad\qquad \boldsymbol{n}_6 = R_z\left(\frac{-\pi}{3}\right)\boldsymbol{n}_1 \tag{23}$$

$$\boldsymbol{n}_7 = P_{1,6;1,12} + k_7\boldsymbol{u}_{1,1;1,12}, \qquad\qquad \boldsymbol{n}_8 = R_z\left(\frac{-\pi}{6} + \sigma\right)R_y(\pi)\,\boldsymbol{n}_7, \tag{24}$$

$$\boldsymbol{n}_{10} = P_{1,7;1,12} + k_{10}\boldsymbol{u}_{1,1;1,7}, \qquad\qquad \boldsymbol{n}_9 = R_z\left(\frac{\pi}{6} + \sigma\right)R_y(\pi)\,\boldsymbol{n}_{10}. \tag{25}$$

for some parameters $k_i, i = 1\ldots 8$. The nodes of the reference face of type 2 are then given by (Figure 4):

$$\boldsymbol{m}_{1+2i} = R_z(\frac{i\pi}{3})\,\boldsymbol{n}_4, \quad \boldsymbol{m}_{2+2i} = R_z(\frac{i\pi}{3})\,\boldsymbol{n}_3 \quad i = 0\ldots 5. \tag{26}$$

(a) (b)
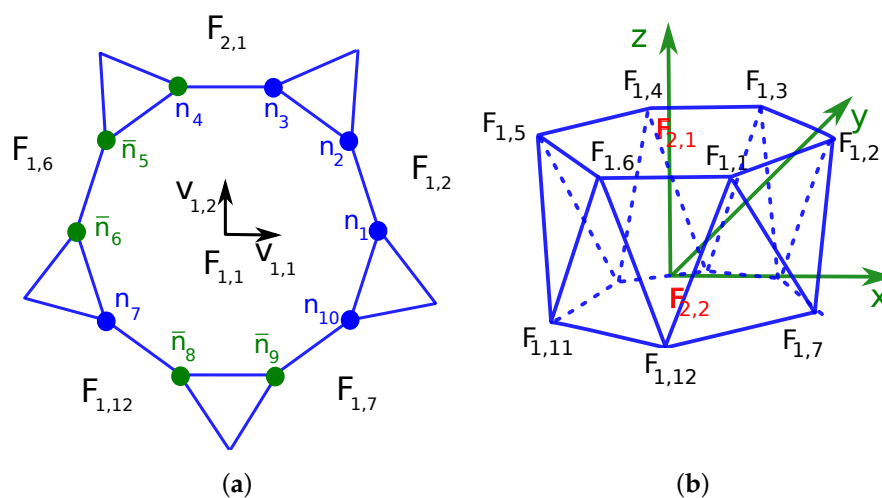
Figure 4. Parametrization of the hexagonal anti-prism p-cage.

The optimization parameters are θ, σ, S_1, S_2, k_1, k_2, k_3, k_4, k_7, and k_{10}, as well as the coordinates of the non-shared vertices within the plane of the faces for both reference faces.

For the optimization to work well, it helps to start from a reasonable initial configuration. We notice that the ten shared edges between the reference face and its five neighbors form a pentagon and we can easily determine the coordinates of its vertices. As an initial configuration, we can locate the shared vertices so that the edges of the pentagon are split into three equal parts. The unshared vertices can then be placed equally spaced between these vertices. This is done explicitly in the code supplied on Zenodo. For the other parameters, we chose as initial values $\theta = 20°$, $\phi = \sigma = 0$, and $S_1 = S_2 = 20$ (this latter value was chosen so that the edge lengths are of order 1).

4.2. TTP6

The underlying symmetry of the TTP6 p-cage is that of a truncated tetrahedron. We have oriented the tetrahedron as depicted in Figure 5.

(**a**) (**b**)
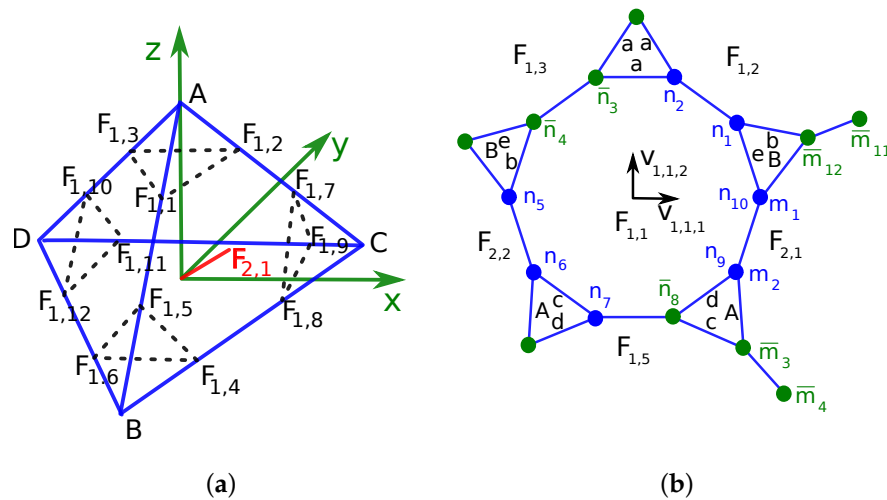
Figure 5. Parametrization of the truncated tetrahedron TTP6 p-cage. (**a**) Truncated tetrahedron vectors. (**b**) Mapping of vertices.

The coordinates of the vertices of the centered tetrahedron are as follows:

$$A = (0,0,1), \quad B = (0, -\frac{\sqrt{8}}{3}, -\frac{1}{3}), \quad C = (\sqrt{\frac{2}{3}}, \frac{\sqrt{2}}{3}, -\frac{1}{3}), \quad D = (-\sqrt{\frac{2}{3}}, \frac{\sqrt{2}}{3}, -\frac{1}{3}), \tag{27}$$

while the centers of the reference faces are given by the following:

$$F_{2,1} = \frac{A+B+C}{3} = (\sqrt{\frac{2}{27}}, -\frac{\sqrt{2}}{9}, \frac{1}{9}), \qquad F_{1,1} = A + \frac{B-A}{3} = \left(0, -\frac{\sqrt{8}}{9}, \frac{5}{9}\right), \tag{28}$$

and the rotations linking the faces are as follows:

$$\mathcal{R}_{1,2} = R_z(\frac{2\pi}{3}), \qquad\qquad \mathcal{R}_{1,3} = R_z(\frac{4\pi}{3}),$$

$$\mathcal{R}_{1,1+j+3i} = R_{F_{2,1}}(\frac{i\,2\pi}{3})R_z(\frac{j2\pi}{3}), \qquad \mathcal{R}_{1,10+j} = R_{F_{2,2}}(\frac{2\pi}{3})R_z(\frac{j2\pi}{3}), \qquad j = 0,1,2,\ i = 1,2$$

$$\mathcal{R}_{2,2} = R_z(\frac{4\pi}{3}), \qquad\qquad \mathcal{R}_{2,3} = R_z(\frac{2\pi}{3}), \qquad\qquad \mathcal{R}_{2,4} = R_B(\frac{4\pi}{3}). \tag{29}$$

We chose the following vectors to parametrize the reference planes:

$$V_{1,1} = S_1 R_z(\phi)\,(0, -\cos(\theta), \sin(\theta)), \qquad V_{2,1} = S_2 F_{2,1},$$

$$v_{1,1,1} = R_z(\phi)\,(1,0,0), \qquad v_{2,1,1} = \frac{C-B}{|C-B|} = \left(\frac{1}{2}, \frac{\sqrt{3}}{2}, 0\right),$$

$$v_{1,1,2} = R_z(\phi)\,(0, \sin(\theta), \cos(\theta)), \qquad v_{2,1,2} = \frac{F_{2,1}-A}{|F_{2,1}-A|} = \left(\frac{1}{2\sqrt{3}}, -\frac{1}{6}, -\frac{\sqrt{8}}{3}\right), \tag{30}$$

where S_1 and S_2 are scaling parameters. The shared vertices of the reference faces are then given by the following:

$$n_1 = P_{2,1;1,2} + k_1 u_{1,1;1,2}, \qquad n_2 = P_{2,1;1,2} + k_2 u_{1,1;1,2}, \qquad n_3 = R_z\left(\frac{-2\pi}{3}\right) n_2,$$

$$n_4 = R_z\left(\frac{-2\pi}{3}\right) n_1, \qquad n_5 = P_{1,3;2,2} + k_5 u_{1,1;2,2}, \qquad n_6 = P_{1,3;1,2,2} + k_6 u_{1,1;2,2},$$

$$n_7 = P_{2,2;1,5} + k_7 u_{1,1;1,5}, \qquad n_8 = R_{F_1}\left(\frac{2\pi}{3}\right) R_z(\frac{2\pi}{3}) n_7, \qquad n_9 = P_{1,5;2,1} + k_9 u_{1,1;2,1},$$

$$n_{10} = P_{1,5;2,1} + k_{10} u_{1,1;2,1}, \qquad m_1 = n_{10}, \ m_2 = n_9, \qquad m_3 = R_{F_{2,1}}\left(\frac{2\pi}{3}\right) R_z(\frac{2\pi}{3}) n_6,$$

$$m_4 = R_{F_{2,1}}\left(\frac{2\pi}{3}\right) R_z(\frac{2\pi}{3}) n_5, \qquad m_i = R_{F_{2,1}}(\frac{2\pi}{3}) m_{i-4} \qquad\qquad i = 5 \dots 12. \tag{31}$$

The optimization parameters are θ, ϕ, S_1, S_2, k_1, k_2, k_5, k_6, k_7, k_9, and k_{10}, as well as the planar coordinates of the non-shared vertices for both reference faces. As initial parameter values we have used $\theta = \arccos(\sqrt{8/33})$, $\phi = 0$, $S_1 = 3.75$, and $S_2 = 9.375$. The other parameters are determined as described in the HAP6 section.

4.3. TOP6

The underlying symmetry of the TOP6 p-cage is that of a truncated octahedron. We orient the octahedron as depicted in Figure 6.

For the vectors normal to the reference faces we use the following:

$$F_{1,1} = (0, -\cos(\theta), \sin(\theta)), \qquad\qquad F_{2,1} = \left(\frac{1}{\sqrt{3}}, -\frac{1}{\sqrt{3}}, \frac{1}{\sqrt{3}}\right) \tag{32}$$

and the rotations linking the faces to the reference faces are as follows:

$$\mathcal{R}_{1,2} = R_z\left(\frac{\pi}{2}\right), \qquad\qquad \mathcal{R}_{1,3} = R_z(\pi), \ \mathcal{R}_{1,4} = R_z\left(\frac{3\pi}{2}\right),$$

$$\mathcal{R}_{2,2} = R_z\left(\frac{\pi}{2}\right), \qquad\qquad \mathcal{R}_{2,3} = R_z(\pi), \ \mathcal{R}_{2,4} = R_z\left(\frac{3\pi}{2}\right),$$

$$\mathcal{R}_{1,4+i} = R_x\left(\frac{\pi}{2}\right) R_z\left(\frac{(i-1)\pi}{2}\right), \qquad\qquad \mathcal{R}_{1,8+i} = R_x(\pi) R_z\left(\frac{(i-1)\pi}{2}\right), \ i = 1 \dots 4$$

$$\mathcal{R}_{1,12+i} = R_x\left(\frac{3\pi}{2}\right) R_z\left(\frac{(i-1)\pi}{2}\right), \qquad\qquad \mathcal{R}_{1,16+i} = R_y\left(\frac{\pi}{2}\right) R_z\left(\frac{(i-1)\pi}{2}\right), \ i = 1 \dots 4$$

$$\mathcal{R}_{1,20+i} = R_y\left(\frac{3\pi}{2}\right) R_z\left(\frac{(i-1)\pi}{2}\right), \qquad\qquad \mathcal{R}_{2,4+i} = R_x(\pi) R_z\left(\frac{(i-1)\pi}{2}\right), \ i = 1 \dots 4. \tag{33}$$

We chose the following vectors to parametrize the reference plane:

$$V_{1,1} = S_1 R_z(\phi) F_{1,1}, \quad v_{1,1,1} = R_z(\phi) (1,0,0),$$

$$v_{1,1,2} = R_z(\phi) (v_{1,1,1} \times V_{1,1}) = R_z(\phi) (0, \sin(\theta), \cos(\theta)),$$

$$V_{2,1} = S_2 F_{2,1}, \quad v_{2,1,1} = \left(\frac{1}{\sqrt{2}}, \frac{1}{\sqrt{2}}, 0\right), \quad v_{2,1,2} = v_{1,1,1} \times V_{2,1} = \left(-\frac{1}{\sqrt{6}}, \frac{1}{\sqrt{6}}, \sqrt{\frac{2}{3}}\right), \tag{34}$$

where S_1 and S_2 are scaling parameters.

The shared vertices of the reference faces are then given by the following:

$$n_1 = P_{2,1;1,2} + k_1 u_{1,1;1,2}, \qquad n_2 = P_{2,1;1,2} + k_2 u_{1,1;1,2}, \qquad n_3 = R_z\left(\frac{-\pi}{2}\right)n_2,$$

$$n_4 = R_z\left(\frac{-\pi}{2}\right)n_1, \qquad n_5 = P_{1,4;2,4} + k_5 u_{1,1;2,4}, \qquad n_6 = P_{1,4;1,2,4} + k_6 u_{1,1;2,4},$$

$$n_7 = P_{2,4;1,7} + k_7 u_{1,1;1,7}, \qquad n_8 = R_x\left(\frac{\pi}{2}\right)R_z(\pi)n_7, \qquad n_9 = P_{1,7;2,1} + k_9 u_{1,1;2,1},$$

$$n_{10} = P_{1,7;2,1} + k_{10} u_{1,1;2,1}, \qquad m_1 = n_{10}, \quad m_2 = n_9, \qquad m_3 = R_{F_{2,1}}\left(\frac{2\pi}{3}\right)R_z(\frac{\pi}{2})n_6,$$

$$m_4 = R_{F_{2,1}}\left(\frac{2\pi}{3}\right)R_z(\frac{\pi}{2})n_5, \qquad m_i = R_{F_{2,1}}(\frac{2\pi}{3})m_{i-4}, \qquad i = 5 \dots 12. \tag{35}$$

The optimization parameters are θ, ϕ, S_1, S_2, k_1, k_2, k_5, k_6, k_7, k_9, and k_{10}, as well as the planar coordinates of the non-shared vertices for both reference faces. As initial parameter values we chose $\theta = 65°$, $\phi = 0$, and $S_1 = S_2 = 4.7$. The other parameters are determined as described in the `HAP6` section.

(**a**)   (**b**)
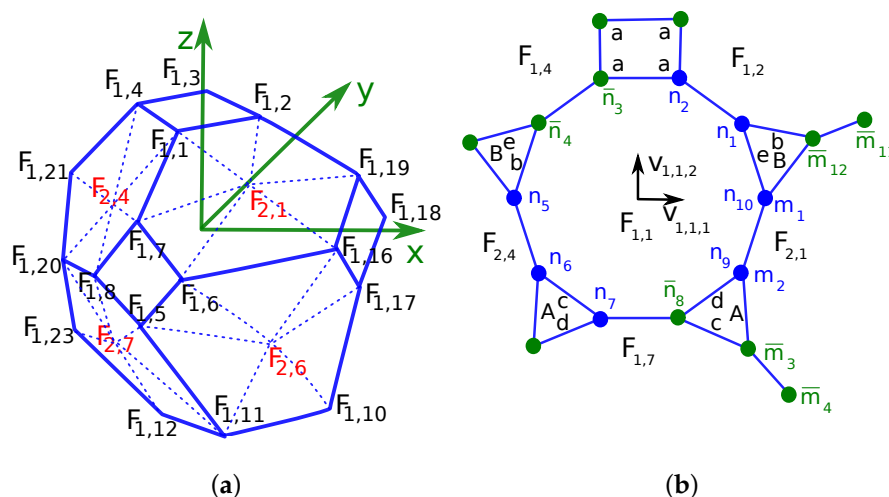
Figure 6. Parametrization of the truncated tetrahedron TOP6 p-cage. (**a**) Truncated tetrahedron vectors. (**b**) Mapping of vertices.

4.4. PD

The underlying symmetry of the `PD` p-cage is that of the dual of a truncated icosahedron. The pentagons sit on the vertices of the icosahedron while the hexagon are placed at the centers of the triangular faces of the icosahedron (Figure 7).

The coordinates of the icosahedron are given by the coordinates of three perpendicular golden ratio rectangles as follows:

$$(0, \pm 1, \pm\varphi), \quad (\pm\varphi, 0, \pm 1,) \quad (\pm 1, \pm\varphi, 0), \tag{36}$$

where $\varphi = (1 + \sqrt{5})/2$ is the golden ratio. The type 1 faces are placed on the vertices of the icosahedron, while the type 2 faces are placed at the center of the icosahedron faces as follows:

$$F_{1,1} = (0, -1, \varphi), \quad F_{2,1} = (F_{1,1} + F_{1,2} + F_{1,6})/3 = (\frac{\varphi}{3}, 0, \frac{1 + 2\varphi}{3}). \tag{37}$$

Defining

$$g = F_{11} \times e_x = (0, \phi_g, 1), \tag{38}$$

the rotations linking the faces to the reference faces are as follows:

$$\mathcal{R}_{1,2} = R_z(\pi), \qquad \mathcal{R}_{1,2+i} = R_{F_{1,1}}\left(i\frac{2\pi}{5}\right)R_z(\pi), \quad i = 1\ldots4$$

$$\mathcal{R}_{1,6+i} = R_g(\pi)\mathcal{R}_{1,i}, \quad i = 1\ldots6 \qquad \mathcal{R}_{2,1+i} = R_{F_{1,1}}\left(i\frac{2\pi}{5}\right), \quad i = 1\ldots4$$

$$\mathcal{R}_{2,5+i} = R_g(\pi), \quad i = 1\ldots5$$

$$\mathcal{R}_{2,11} = R_{F_{2,1}}\left(\frac{4\pi}{5}\right), \quad \mathcal{R}_{2,12+1} = R_{F_{2,1}}\left(i\frac{2\pi}{5}\right)R_{F_{2,1}}\left(\frac{4\pi}{5}\right), \quad i = 1\ldots4,$$

$$\mathcal{R}_{2,12} = R_{F_{2,1}}\left(\frac{6\pi}{5}\right), \quad \mathcal{R}_{2,16+1} = R_{F_{2,1}}\left(i\frac{2\pi}{5}\right)R_{F_{2,1}}\left(\frac{6\pi}{5}\right), \quad i = 1\ldots4. \tag{39}$$

We chose the following vectors to parametrize the reference plane:

$$V_{1,1} = S_1\,F_{1,1}, \quad v_{1,1,1} = (1,0,0), \quad v_{1,1,2} = v_{1,1,1} \times V_{1,1} = \frac{\sqrt{2}}{\sqrt{\sqrt{5}+5}}(0,\varphi,1),$$

$$V_{2,1} = S_2\,F_{2,1}, \quad v_{2,1,1} = (0,1,0), \quad v_{2,1,2} = v_{1,1,1} \times V_{2,1} = \frac{\sqrt{6}}{3\sqrt{3\sqrt{5}+7}}\left(-\sqrt{5}-2,0,\varphi\right), \tag{40}$$

where S_1 and S_2 are scaling parameters.

The shared vertices of the reference faces are given by the following:

$$n_1 = P_{2,5;2,1} + k_1 u_{1,1;2,1}, \qquad n_2 = P_{2,5;2,1} + k_2 u_{1,1;2,1},$$

$$n_{1+2i} = R_{F_{1,1}}\left(\frac{i\,2\pi}{5}\right)n_1, \qquad n_{2+2i} = R_{F_{1,1}}\left(\frac{i\,2\pi}{5}\right)n_2, \quad i = 1\ldots4$$

$$m_1 = n_2, \qquad m_2 = n_1,$$

$$m_{1+2i} = R_{F_{2,1}}\left(\frac{i\,\pi}{3}\right)m_1, \qquad m_{2+2i} = R_{F_{2,1}}\left(\frac{i\,\pi}{3}\right)m_2, \quad i = 1\ldots5. \tag{41}$$

The optimization parameters are S_1, S_2, k_1, k_2, k_3, and k_4, as well as the planar coordinates of the non-shared vertices for both reference faces. As initial parameters values we chose $S_1 = 14.14$ and $S_2 = 18$, while the other parameters are determined as described in the HAP6 section.
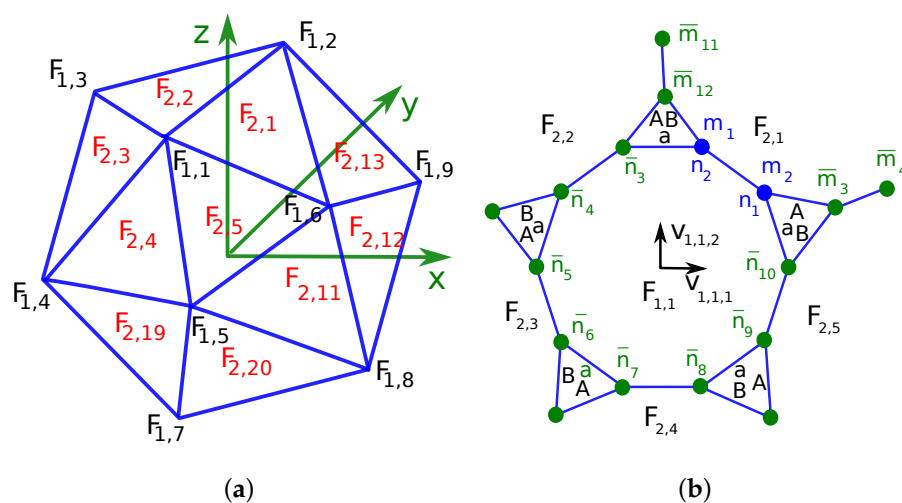
Figure 7. Parametrization of the Pentakis dodecahedron PD p-cage. (**a**) Pentakis dodecahedron vectors. (**b**) Mapping of vertices.

4.5. IP5

The underlying symmetry of the IP5 p-cage is that of the dual of the icosidodecahedron (Figure 8).
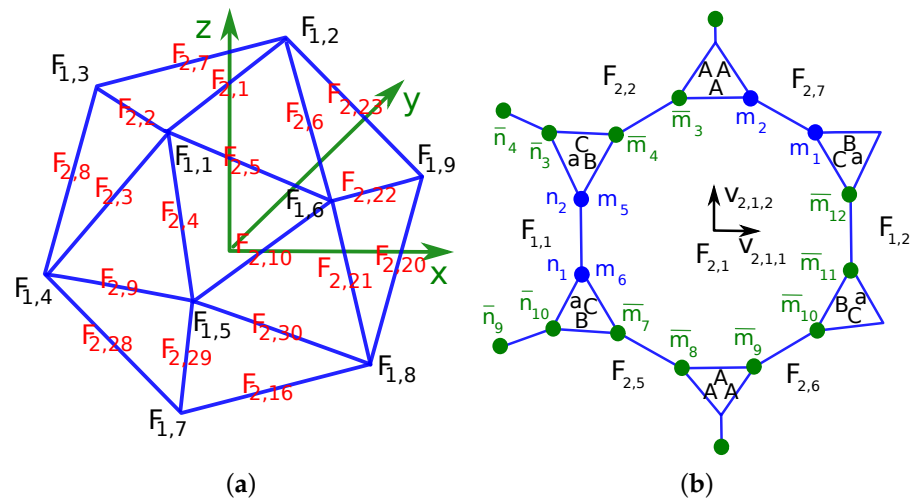
Figure 8. Parametrization of the icosidodecahedron with a pyramid on the pentagonal faces' p-cage. (**a**) Icosidodecahedron vectors. (**b**) Mapping of vertices.

The type 1 faces are placed at the centers of the pentagons of the icosidodecahedron. The vectors pointing to these centers correspond to the 12 vertices of the icosahedron. The type 2 hexagonal faces are placed on the vertices of the icosidodecahedron, which correspond to the midpoint of icosidodecahedron edges:

$$\boldsymbol{F}_{1,1} = (0, -1, \varphi), \qquad \boldsymbol{F}_{1,2} = R_z(\pi)\boldsymbol{F}_{1,1} = (0, 1, \varphi), \qquad \boldsymbol{F}_{2,1} = \frac{1}{2}(\boldsymbol{F}_{1,1} + \boldsymbol{F}_{1,2}) = (0, 0, \varphi). \tag{42}$$

The rotations linking the faces to the reference faces are as follows:

$$\mathcal{R}_{1,2} = R_z(\pi), \qquad \mathcal{R}_{1,2+i} = R_{F_{1,1}}\left(i\frac{2\pi}{5}\right)R_z(\pi), \quad i = 1\dots 4$$

$$\mathcal{R}_{1,6+i} = R_g(\pi)\,\mathcal{R}_{1,i} \quad i = 1\dots 6, \qquad \mathcal{R}_{2,1+i} = R_{F_{1,1}}\left(i\frac{i2\pi}{5}\right), \quad i = 1\dots 4$$

$$\mathcal{R}_{2,6} = R_{G_1}\left(\frac{4\pi}{3}\right), \qquad \mathcal{R}_{2,6+i} = R_{F_{1,1}}\left(i\frac{2\pi}{5}\right)\mathcal{R}_{2,6} \quad i = 1\dots 4$$

$$\mathcal{R}_{2,10+i} = R_g(\pi)\,\mathcal{R}_{2,i}, \quad i = 1\dots 10$$

$$\mathcal{R}_{2,21} = R_{F_{1,6}}\left(\frac{6\pi}{5}\right)\mathcal{R}_{2,6}, \qquad \mathcal{R}_{2,21+2i} = R_{F_{1,1}}\left(i\frac{2\pi}{5}\right)\mathcal{R}_{2,21},$$

$$\mathcal{R}_{2,22} = R_{F_{1,6}}\left(\frac{8\pi}{5}\right)\mathcal{R}_{2,6}, \qquad \mathcal{R}_{2,22+2i} = R_{F_{1,1}}\left(i\frac{2\pi}{5}\right)\mathcal{R}_{2,22}, \tag{43}$$

where $\boldsymbol{g} = \boldsymbol{F}_{11} \times \boldsymbol{e}_y$ and

$$\boldsymbol{F}_{1,2} = R_z(\pi)\boldsymbol{F}_{1,1} = (0, 1, \varphi), \qquad \boldsymbol{F}_{1,6} = (\varphi, 0, 1,) \qquad \boldsymbol{G}_1 = \frac{1}{3}(\boldsymbol{F}_{1,1} + \boldsymbol{F}_{1,2} + \boldsymbol{F}_{1,6}). \tag{44}$$

We chose the following vectors to parametrize the reference plane:

$$\boldsymbol{V}_{1,1} = S_1\,\boldsymbol{F}_{1,1}, \quad \boldsymbol{v}_{1,1,1} = (1, 0, 0), \quad \boldsymbol{v}_{1,1,2} = \boldsymbol{v}_{1,1,1} \times \boldsymbol{V}_{1,1} = \frac{\sqrt{2}}{\sqrt{\sqrt{5}+5}}(0, \varphi, 1),$$

$$\boldsymbol{V}_{2,1} = S_2\,\boldsymbol{F}_{2,1}, \quad \boldsymbol{v}_{2,1,1} = (0, 1, 0), \quad \boldsymbol{v}_{2,1,2} = (-1, 0, 0). \tag{45}$$

where S_1 and S_2 are scaling parameters.

The shared vertices of the reference faces are given by the following:

$$m_1 = Q_{1,2;2,7} + k_1 u_{2,1;2,7}, \qquad m_2 = Q_{1,2;2,7} + k_2 u_{2,1;2,7}, \qquad m_3 = R_{G_2}\left(\frac{4\pi}{3}\right)m_2,$$

$$m_4 = R_{G_2}\left(\frac{4\pi}{3}\right)m_1, \qquad m_5 = Q_{2,2;1,1} + k_5 u_{2,1;1,1}, \qquad m_6 = Q_{2,2;1,1} + k_6 u_{2,1;1,1},$$

$$m_{6+i} = R_{F_{2,1}}(\pi)m_i, \qquad i = 1\ldots 6,$$

$$n_1 = m_6, \qquad n_{1+2i} = R_{F_{1,1}}\left(i\frac{2\pi}{5}\right)n_1, \qquad i = 1\ldots 4.$$

$$n_2 = m_5, \qquad n_{2+2i} = R_{F_{1,1}}\left(i\frac{2\pi}{5}\right)n_2, \qquad i = 1\ldots 4. \tag{46}$$

The optimization parameters are S_1, S_2, k_1, k_2, k_5, and k_6, as well as the planar coordinates of the non-shared vertices for both reference faces. As initial parameters values we choose $S_1 = 3$ and $S_2 = 3.5$, while the other parameters are determined as described in the HAP6 section.

4.6. SDP5

The underlying symmetry of the SDP5 p-cage is that of the snub dodecahedron (Figure 9).

(a)   (b)   (c)
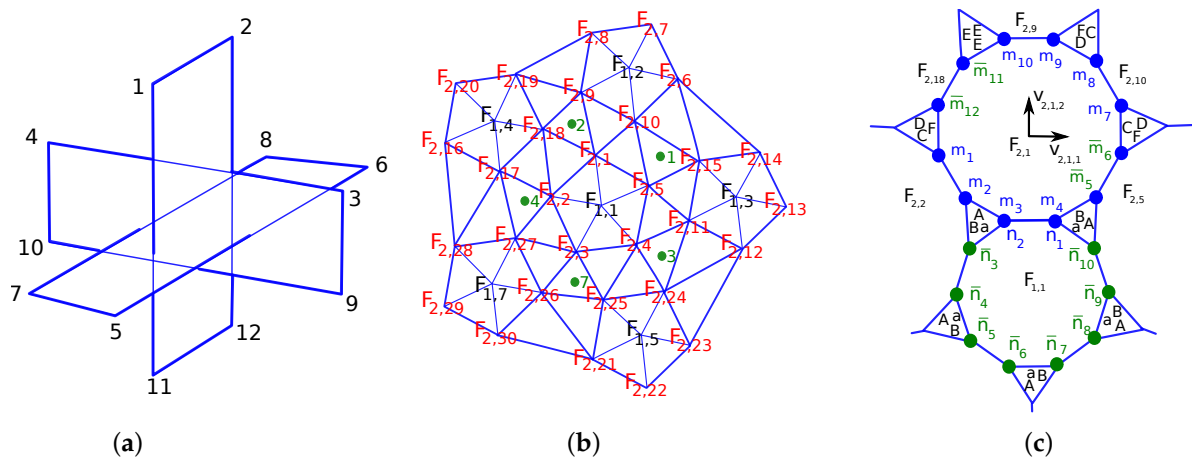
Figure 9. Parametrization of the cage built on a snub dodecahedron with pyramids on the pentagons' p-cage. (**a**) Dodecahedron node numbering. (**b**) Partial face labeling. The green dots correspond to the vectors $A_{v,i}$. (**c**) Mapping of vertices.

The normal vectors to the reference planes are as follows:

$$F_{1,1} = (0, -1, \varphi), \quad F_{2,1} = (0, 0, 1), \tag{47}$$

Defining $G_{i,j,k} = (F_{1,i} + F_{1,j} + F_{1,k})/3$, the rotation axe vectors are as follows:

$$A_{v,1} = G_{1,2,3} = \left(\frac{\varphi}{3}, 0, \frac{2\varphi+1}{3}\right), \qquad A_{v,3} = G_{1,3,5} = \left(\frac{\varphi^2}{3}, -\frac{\varphi^2}{3}, \frac{\varphi^2}{3}\right),$$

$$A_{v,4} = G_{1,4,7} = \left(-\frac{\varphi^2}{3}, -\frac{\varphi^2}{3}, \frac{\varphi^2}{3},\right), \qquad A_{v,5} = G_{2,3,6} = \left(\frac{\varphi^2}{3}, \frac{\varphi^2}{3}, \frac{\varphi^2}{3},\right),$$

$$A_{v,8} = G_{2,6,8} = \left(0, \frac{2\varphi+1}{3}, \frac{\varphi}{3}\right), \qquad A_{v,9} = G_{3,5,9} = \left(\frac{2\varphi+1}{3}, -\frac{\varphi}{3}, 0\right),$$

$$A_{v,14} = G_{7,10,11} = \left(-\frac{\varphi^2}{3}, -\frac{\varphi^2}{3}, -\frac{\varphi^2}{3}\right), \qquad A_{v,15} = G_{6,9,12} = \left(\frac{\varphi^2}{3}, \frac{\varphi^2}{3}, -\frac{\varphi^2}{3}\right). \tag{48}$$

The rotations linking the faces to the reference faces are given by the following:

$$\mathcal{R}_{1,2} = R_{A_{v,1}}\left(\frac{4\pi}{3}\right), \qquad \mathcal{R}_{1,3} = R_{A_{v,1}}\left(\frac{2\pi}{3}\right), \qquad \mathcal{R}_{1,4} = R_{A_{v,4}}\left(\frac{2\pi}{3}\right),$$

$$\mathcal{R}_{1,5} = R_{A_{v,3}}\left(\frac{2\pi}{3}\right), \qquad \mathcal{R}_{1,6} = R_{A_{v,5}}\left(\frac{4\pi}{3}\right)\mathcal{R}_{1,2}, \qquad \mathcal{R}_{1,7} = R_{A_{v,4}}\left(\frac{4\pi}{3}\right),$$

$$\mathcal{R}_{1,8} = R_{A_{v,8}}\left(\frac{4\pi}{3}\right)\mathcal{R}_{1,2}, \qquad \mathcal{R}_{1,9} = R_{A_{v,9}}\left(\frac{4\pi}{3}\right)\mathcal{R}_{1,3}, \qquad \mathcal{R}_{1,10} = R_{A_{v,14}}\left(\frac{2\pi}{3}\right)\mathcal{R}_{1,7},$$

$$\mathcal{R}_{1,11} = R_{A_{v,14}}\left(\frac{4\pi}{3}\right)\mathcal{R}_{1,7}, \qquad \mathcal{R}_{1,12} = R_{A_{v,15}}\left(\frac{4\pi}{3}\right)\mathcal{R}_{1,6},$$

$$\mathcal{R}_{2,1+5j+i} = \mathcal{R}_{1,j+1}\, R_{F_{1,1}}\left(i\frac{2\pi}{3}\right), \qquad\qquad i = 0\dots4, j = 0\dots11. \tag{49}$$

We chose the following vectors to parametrize the reference plane:

$$\boldsymbol{V}_{1,1} = S_1\,\boldsymbol{F}_{1,1} = S_1\,(0,-1,\varphi),\ \boldsymbol{v}_{1,1,1} = \hat{\boldsymbol{e}}_x, \quad \boldsymbol{v}_{1,1,2} = \left(0, \varphi\frac{\sqrt{2}}{\sqrt{\sqrt{5}+5}}, \frac{\sqrt{2}}{\sqrt{\sqrt{5}+5}}\right),$$

$$\boldsymbol{V}_{2,1} = S_2\,R_z(\phi)\,R_x(\theta)\,\hat{\boldsymbol{e}}_z, \quad \boldsymbol{v}_{2,1,1} = R_z(\phi)\,R_x(\theta)\hat{\boldsymbol{e}}_x, \quad \boldsymbol{v}_{2,1,2} = R_z(\phi)\,R_x(\theta)\hat{\boldsymbol{e}}_y. \tag{50}$$

With these we have the following:

$$\boldsymbol{m}_1 = Q_{2,18;2,2} + k_1\boldsymbol{u}_{2,1;2,2}, \qquad \boldsymbol{m}_2 = Q_{2,18;2,2} + k_2\boldsymbol{u}_{2,1;2,2}, \qquad \boldsymbol{m}_3 = Q_{2,2;1,1} + k_3\boldsymbol{u}_{2,1;1,1},$$

$$\boldsymbol{m}_4 = Q_{2,2;1,1} + k_4\boldsymbol{u}_{2,1;1,1}, \qquad \boldsymbol{m}_5 = R_{A_{1,1}}\left(\frac{8\pi}{5}\right)\boldsymbol{m}_2, \qquad \boldsymbol{m}_6 = R_{A_{1,1}}\left(\frac{8\pi}{5}\right)\boldsymbol{m}_1,$$

$$\boldsymbol{m}_7 = Q_{2,5;2,10} + k_7\boldsymbol{u}_{2,1;2,10}, \qquad \boldsymbol{m}_8 = Q_{2,5;2,10} + k_8\boldsymbol{u}_{2,1;2,10}, \qquad \boldsymbol{m}_9 = Q_{2,10;2,9} + k_9\boldsymbol{u}_{2,1;2,9},$$

$$\boldsymbol{m}_{10} = Q_{2,10;2,9} + k_{10}\boldsymbol{u}_{2,1;2,9}, \qquad \boldsymbol{m}_{11} = R_{F_{1,1}}\left(\frac{4\pi}{5}\right)\boldsymbol{m}_{10}, \qquad \boldsymbol{m}_{12} = R_{F_{1,1}}\left(\frac{4\pi}{5}\right)\boldsymbol{m}_9,$$

$$\boldsymbol{n}_1 = \boldsymbol{m}_4, \qquad \boldsymbol{n}_{1+2i} = R_{F_{1,1}}\left(i\frac{2\pi}{5}\right)\boldsymbol{n}_1, \qquad i = 1\dots4.$$

$$\boldsymbol{n}_2 = \boldsymbol{m}_3, \qquad \boldsymbol{n}_{2+2i} = R_{F_{1,1}}\left(i\frac{2\pi}{5}\right)\boldsymbol{n}_2, \qquad i = 1\dots4. \tag{51}$$

The optimization parameters are Θ, ϕ, S_1, S_2, k_1, k_2, k_3, k_4, k_7, k_8,k_9, and k_{10}, as well as the planar coordinates of the non-shared vertices for both reference faces. As initial parameter values we use $\theta = 5°$, $\phi = -25°$, $S_1 = 4$, and $S_2 = 7.5$, while the other parameters are determined as described in the HAP6 section.

5. Results

We used a computer program to optimize (3) for each configuration described above with the restrictions that each face contributes up to three of its edges to each hole. That restriction was chosen to avoid p-cages with very large holes. A python program was used to generate all the combinations of the labels a to e and A to F satisfying (1), where each label may take the values 1, 2, or 3, which led to over half a million configurations to optimize. We used a simulated annealing method to minimize (3) for 200 values of c_l and c_a, with the constraint $c_l + c_a = 2$, taking $c_c = c_{pc} = 500$ and then selected the p-cage with the smallest value of $\max(\Delta_l, \Delta_a)$.

The p-cages are named according to the graphs they are build from, the size of the face, and the number of edges contributing to the holes, as follows: $GRAPH\_PP_1\_PP_2\_a\_b\_c\_d\_e$-$A\_B\_C\_D\_E\_F$ where the italic symbols are replaced by their value. To avoid very long names, we also use a simplification when n successive hole-edge labels have the same values, α, where we replace the sequence $\alpha\_\alpha\_\dots\alpha$ by nxα. Thus, for exam-

ple, `IP5_P10_P12_5x1-6x1` is equivalent to `IP5_P10_P12_1_1_1_1_1-1_1_1_1_1_1`, or `SDP5_P15_P21_5x2-2x2_2x3_2_3` is equivalent to `SDP5_P15_P21_2_2_2_2_2_2-2_2_3_3_2_3`.

Our first result was that none of these configurations lead to regular p-cages. The best `HAP6` p-cage has a deformation just under 5%. The two type 2 faces, at the top and bottom of the p-cage, are surrounded by two rings of five type 1 faces joined together (Figure 10a).

The least deformed p-cages are of the type `PD`: `PD_P20_P24_5x3-6x3` has the deformations $\Delta_l = 0.0084$, $\Delta_a = 0.0084$, and `PD_P10_P12_5x1-6x1`, which is similar in structure but with smaller polygons has deformations just exceeding 1%: $\Delta_l = 0.0109$ and $\Delta_a = 0.0109$ (Figure 10b–d).

The `IP5` p-cages are made out of respectively 12 and 36 faces of types 1 and 2. The p-cage `IP5_P10_P12_5x1-6x1` is nearly regular with the deformations $\Delta_l = 0.0161$ and $\Delta_a = 0.0161$. (Figure 10e).

(**a**)　　　　(**b**)　　　　(**c**)　　　　(**d**)

(**e**)　　　　(**f**)　　　　(**g**)　　　　(**h**)
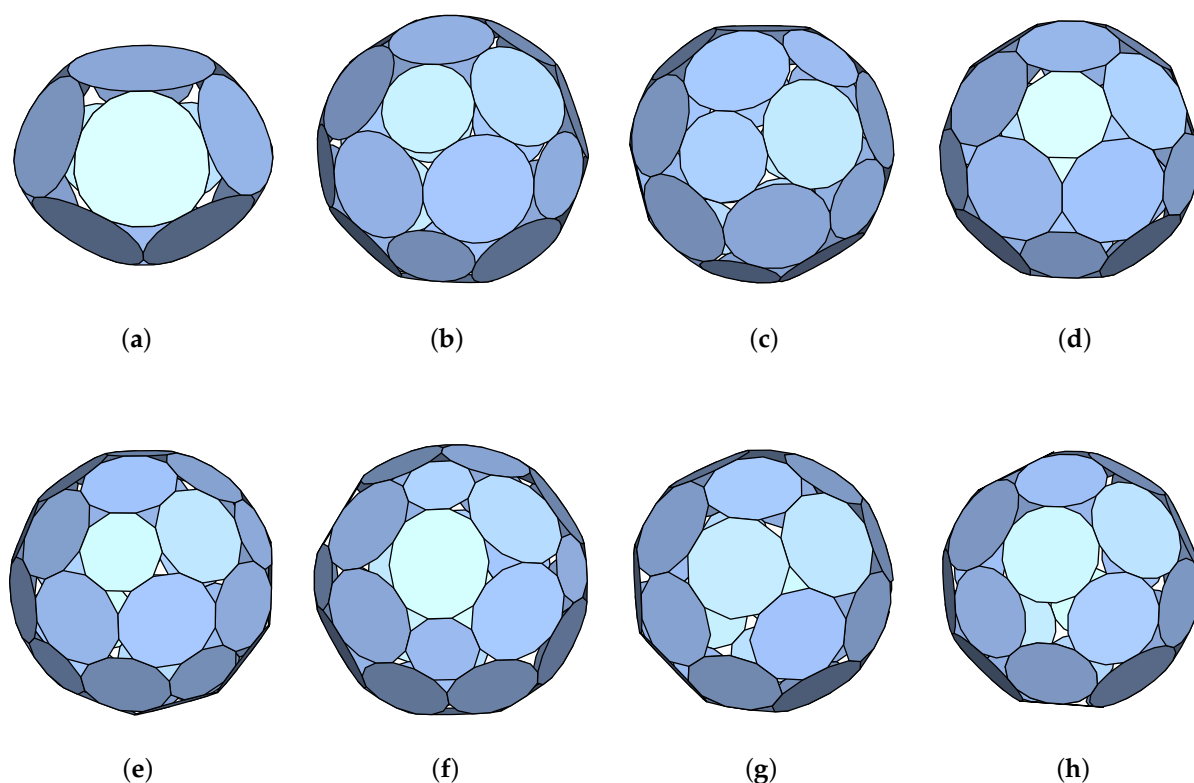
Figure 10. Some of the least irregular p-cages: (**a**) `HAP6_P20_P24_5x3-6x3_c10` $\Delta_l = 0.0474$, $\Delta_a = 0.0474$, (**b**) `PD_P20_P24_5x3-6x3` $\Delta_l = 0.0084$, $\Delta_a = 0.0084$, (**c**) `PD_P15_P18_5x2-6x2` $\Delta_l = 0.0096$, $\Delta_a = 0.0096$, (**d**) `PD_P10_P12_5x1-6x1` $\Delta_l = 0.0109$, $\Delta_a = 0.0109$, (**e**) `IP5_P10_P12_5x1-6x1` $\Delta_l = 0.0161$, $\Delta_a = 0.0161$, (**f**) `IP5_P10_P14_5x1-2_2x1_2_2x1` $\Delta_l = 0.0296$, $\Delta_a = 0.0295$, (**g**) `TOP6_P11_P12_2_4x1-6x1` $\Delta_l = 0.0096$, $\Delta_a = 0.0093$, (**h**) `TOP6_P16_P18_3_4x2-6x2` $\Delta_l = 0.0234$, $\Delta_a = 0.0234$.

The p-cage `IP5_P10_P14_5x1-2_2x1_2_2x1` is interesting in that its hole-edge labels are not identical and still it has the relatively small deformations $\Delta_l = 0.0296$ and $\Delta_a = 0.0295$ (Figure 10f). The `TOP6` p-cages are made out of respectively 24 and 8 faces of types 1 and 2. The p-cage `TOP6_P11_P12_2_4x1-6x1` is particularly interesting in that it is made out of the polygons, hendecagons, and dodecagons, from which the nano-cages used, separately, in [2,3] are made. Its deformations are relatively small too, namely $\Delta_l = 0.0096$ and $\Delta_a = 0.0093$ (Figure 10g). The p-cage `TOP6_P16_P18_3_4x2-6x2` is another example of a p-cage with differing hole-edge labels and with still relatively small deformations: $\Delta_l = 0.0234$ and $\Delta_a = 0.0234$ (Figure 10h).

The `TTP6` p-cages are made out of respectively 12 and 4 faces of types 1 and 2. The p-cages `TTP6_P20_P24_5x3-6x3`, `TTP6_P15_P18_5x2-6x2`, and `TTP6_P10_P12_5x1-6x1` all have a similar structure with the respective deformations $\Delta_l = 0.0229$, $\Delta_a = 0.0229$, $\Delta_l = 0.0261$, $\Delta_a = 0.0261$, $\Delta_l = 0.0297$, and $\Delta_a = 0.0297$ (Figure 11a–c).

The `SDP5` p-cages are made out of respectively 12 and 60 faces of types 1 and 2. These are the largest bi-symmetric p-cages with maximal connectivity between faces. The p-cages `SDP5_P20_P24_5x3-6x3`, `SDP5_P15_P18_5x2-6x2`, and `SDP5_P10_P12_5x1-6x1` have a similar structure with the respective deformations $\Delta_l = 0.0212$, $\Delta_a = 0.0211$, $\Delta_l = 0.0261$, $\Delta_a = 0.0261$, $\Delta_l = 0.0326$, and $\Delta_a = 0.0326$ (Figure 11d,f,g). The p-cage `SDP5_P15_P21_5x2-2x2_2x3_2_3` is another example of a p-cage with non-identical hole-edge numbers and relatively small deformations, namely $\Delta_l = 0.0214$ and $\Delta_a = 0.0189$ (Figure 11e).

The `TCM4` p-cages are made out of 24 faces of each type. The configuration `TCM3` leads to 68 p-cages with deformations below 10%, but the least deformed p-cage, `TCM4_P20_P24_5x3-6x3`, has a deformation of over 8%: $\Delta_l = 0.0805$, $\Delta_a = 0.0690$ (Figure 11h). While aesthetically pleasing, it does not constitute a good candidate for a protein cage.
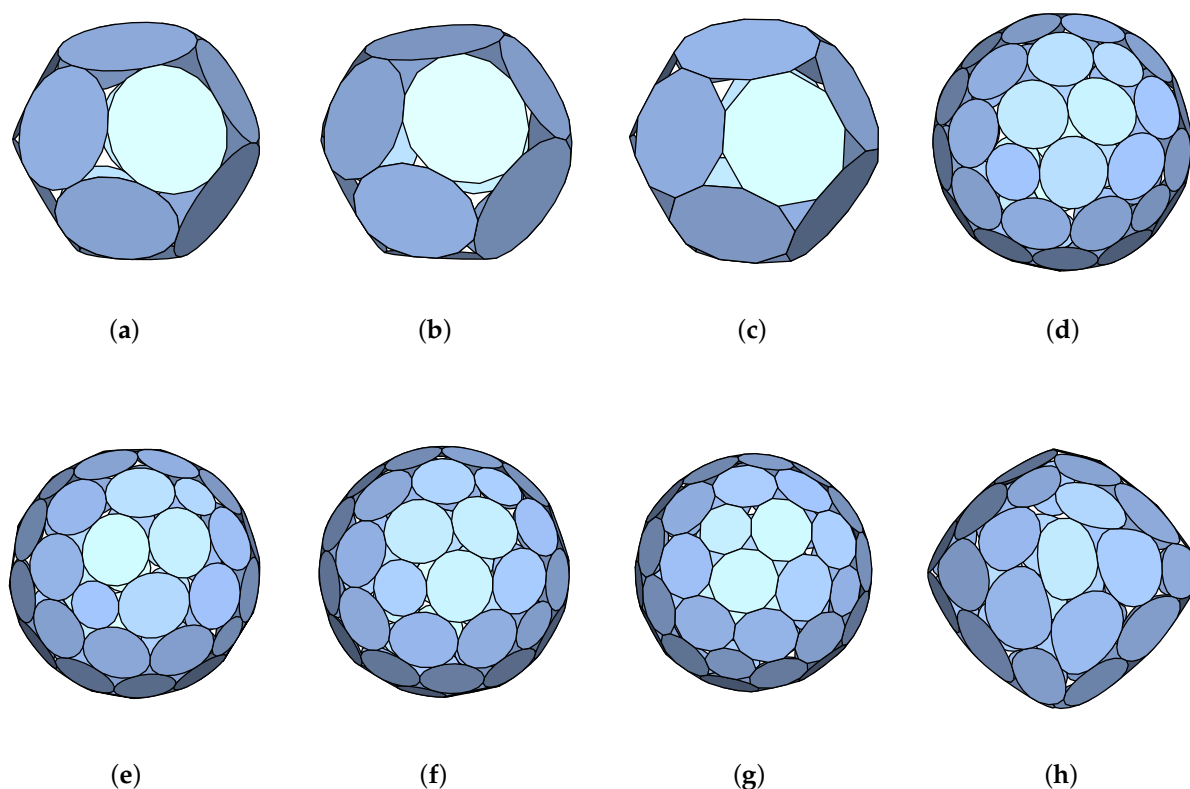
Figure 11. Some of the least irregular p-cages: (**a**) `TTP6_P20_P24_5x3-6x3` $\Delta_l = 0.0229$, $\Delta_a = 0.0229$ (**b**) `TTP6_P15_P18_5x2-6x2` $\Delta_l = 0.0261$, $\Delta_a = 0.0261$ (**c**) `TTP6_P10_P12_5x1-6x1` $\Delta_l = 0.0297$, $\Delta_a = 0.0297$ (**d**) `SDP5_P20_P24_5x3-6x3` $\Delta_l = 0.0212$, $\Delta_a = 0.0211$ (**e**) `SDP5_P15_P21_5x2-2x2_2x3_2_3` $\Delta_l = 0.0214$, $\Delta_a = 0.0189$ (**f**) `SDP5_P15_P18_5x2-6x2` $\Delta_l = 0.0261$, $\Delta_a = 0.0261$ (**g**) `SDP5_P10_P12_5x1-6x1` $\Delta_l = 0.0326$, $\Delta_a = 0.0326$ (**h**) `TCM4_P20_P24_5x3-6x3` $\Delta_l = 0.0805$, $\Delta_a = 0.0690$.

The full list, including figures, of all of the obtained p-cages with deformations not exceeding 10% as well as well as files containing their coordinates are available as Supplementary Materials.

6. Conclusions

In this paper, we have constructed near-miss p-cages made out of two types of faces such that the faces of one family have five neighbors while the others have six. Moreover, each face of a given family can be mapped to any other face of the same family via a rotation automorphism of the p-cage.

We have shown that the p-cages can be constructed by placing the faces on the vertices of the so-called hole-polyhedron, the edges of which describes how the faces are attached to each other. The bi-symmetry of the p-cage and the constraint of each face having five or six neighbors restricts the hole-polyhedron graphs to be one of nine graphs identified in [7]. From these nine hole-polyhedron graphs, two leads to p-cages with deformations exceeding 10% (TTM3 and TOM3 p-cages), while the TCM3 p-cages have quite large deformations exceeding 8%. The other six types of p-cages have much smaller deformations, a number of them being approximately 1%.

Comparing the p-cages we have obtained in this paper with the ones described in our previous work [4–6], we first of all notice that the geometries we have considered do not lead to regular p-cages and that the smallest deformations are of the order of 1%. As some experimentally realized protein cages exhibit deformation of several percentage points, this does not rule these configuration out to be realized experimentally. On the other hand, the p-cages we have described here are made out of a larger number of faces and also have, by design, small holes, making them good candidates for large protein cages.

If we restrict ourselves to a small P, and thus to a small number of hole-edges, the following p-cages are good candidates for artificial protein cages: PD_P10_P12_5x1–6x1 (deformation 1.09%), TOP6_P11_P12_2_4x1–6x1 (deformation 0.096%), IP5_P10_P12_5x1–6x1 (deformation 1.61%), TTP6_P10_P12_5x1–6x1 (deformation 3%), IP5_P10_P14_5x2–2_2x1_2_2x1 (deformation 3%), or SDP5_P10_P24_5x1–6x1 (deformation 3.26%). Hence, each type of p-cage, except possibly HAP6, are potential geometries for good p-cages. Note, that SDP5_P10_P24_5x1–6x1 is the largest of these p-cages, as it is made out of 72 faces. The TTP6 p-cages are the smallest with only 16 faces, the TOP6 and PD p-cages have 32 faces, and the IP5 p-cages have 42.

Abbreviations

The following abbreviation is used in this manuscript:

TRAP   trp RNA-binding attenuation protein.
RNA   Ribonucleic acid: a nucleic acid present in all living cells.
DNA   Deoxyribonucleic acid: a nucleic acid present in all living cells.

References

1. Malay, A.D.; Heddle, J.G.; Tomita, S.; Iwasaki, K.; Miyazaki, N.; Sumitomo, K.; Yanagi, H.; Yamashita, I.; Uraoka, Y. Gold nanoparticle-induced formation of artificial protein capsids. *Nano Lett.* **2012**, *12*, 2056–2059. [CrossRef] [PubMed]
2. Malay, A.D.; Miyazaki, N.; Biela, A.; Chakraborti, S.; Majsterkiewicz, K.; Stupka, I.; Kaplan, C.S.; Kowalczyk, A.; Piette, B.M.; Hochberg, G.K.; et al. An ultra-stable gold-coordinated protein cage displaying reversible assembly. *Nature* **2019**, *569*, 438–442. [CrossRef]
3. Majsterkiewicz, K.; Biela, A.P.; Maity, S.; Sharma, M.; Piette, B.M.; Kowalczyk, A.; Gaweł, S.; Chakraborti, S.; Roos, W.H.; Heddle, J.G. Artificial Protein Cage with Unusual Geometry and Regularly Embedded Gold Nanoparticles. *Nano Lett.* **2022**, *22*, 3187–3195. [CrossRef]
4. Piette, B.M.A.G.; Kowalczyk, A.; Heddle, J.G. Characterization of near-miss connectivity-invariant homogeneous convex polyhedral cages. *Proc. R. Soc. A* **2022**, *478*, 20210679. [CrossRef] [PubMed]
5. Piette, B.M.A.G.; Lukács, A. Near-Miss Symmetric Polyhedral Cage. *Symmetry* **2023**, *15*, 717. [CrossRef]
6. Piette, B.M.A.G.; Lukács, A. Near-Miss Bi-Homogenous Symmetric Polyhedral Cage. *Symmetry* **2023**, *15*, 1804. [CrossRef]
7. Piette, B.M.A.G. Biequivalent Planar Graphs. *Axioms* **2024**, *13*, 437. [CrossRef]
8. Chakraborti, S.; Lin, T.Y.; Glatt, S.; Heddle, J.G. Enzyme encapsulation by protein cages. *RSC Adv.* **2020**, *10*, 13293–13301. [CrossRef]
9. Gao, R.; Tan, H.; Li, S.; Ma, S.; Tang, Y.; Zhang, K.; Zhang, Z.; Fan, Q.; Yang, J.; Zhang, X.E.; et al. A prototype protein nanocage minimized from carboxysomes with gated oxygen permeability. *Proc. Natl. Acad. Sci. USA* **2022**, *119*, e2104964119. [CrossRef] [PubMed]
10. Zhu, J.; Avakyan, N.; Kakkis, A.; Hoffnagle, A.M.; Han, K.; Li, Y.; Zhang, Z.; Choi, T.S.; Na, Y.; Yu, C.J.; et al. Protein Assembly by Design. *Chem. Rev.* **2021**, *12*, 13701–13796. [CrossRef]
11. Lapenta, F.; Aupič, J.; Vezzoli, M.; Strmšek, Ž.; Da Vela, S.; Svergun, D.I.; Carazo, J.M.; Melero, R.; Jerala, R. Self-assembly and regulation of protein cages from pre-organised coiled-coil modules. *Nat. Commun.* **2021**, *12*, 939. [CrossRef]
12. Percastegui, E.G.; Ronson, T.K.; Nitschke, J.R. Design and Applications of Water-Soluble Coordination Cages. *Chem. Rev.* **2020**, *120*, 13480–13544. [CrossRef]
13. Golub, E.; Subramanian, R.H.; Esselborn, J.; Alberstein, R.G.; Bailey, J.B.; Chiong, J.A.; Yan, X.; Booth, T.; Baker, T.S.; Tezcan, F.A. Constructing protein polyhedra via orthogonal chemical interactions. *Nature* **2020**, *578*, 172–176. [CrossRef] [PubMed]
14. Liang, Y.; Furukawa, H.; Sakamoto, K.; Inaba, H.; Matsuura, K. Anticancer Activity of Reconstituted Ribonuclease S-Decorated Artificial Viral Capsid. *ChemBioChem* **2022**, *23*, e202200220. [CrossRef]
15. Olshefsky, A.; Richardson, C.; Pun, S.H.; King, N.P. Engineering Self-Assembling Protein Nanoparticles for Therapeutic Delivery. *Bioconjug. Chem.* **2022**, *33*, 2018–2034. [CrossRef] [PubMed]
16. Luo, X.; Liu, J. Ultrasmall Luminescent Metal Nanoparticles: Surface Engineering Strategies for Biological Targeting and Imaging. *Adv. Sci.* **2022**, *9*, e2103971. [CrossRef] [PubMed]
17. Naskalska, A.; Borzęcka-Solarz, K.; Różycki, J.; Stupka, I.; Bochenek, M.; Pyza, E.; Heddle, J.G. Artificial Protein Cage Delivers Active Protein Cargos to the Cell Interior. *Biomacromolecules* **2021**, *22*, 4146–4154. [CrossRef]
18. Edwardson, T.G.W.; Tetter, S.; Hilvert, D. Two-tier supramolecular encapsulation of small molecules in a protein cage. *Nat. Commun.* **2020**, *11*, 5410. [CrossRef]
19. Stupka, I.; Azuma, Y.; Biela, A.P.; Imamura, M.; Scheuring, S.; Pyza, E.; Woźnicka, O.; Maskell, D.P.; Heddle, J.G. Chemically induced protein cage assembly with programmable opening and cargo release. *Sci. Adv.* **2022**, *8*, eabj9424. [CrossRef]
20. Twarock, R.; Luque, A. Structural puzzles in virology solved with an overarching icosahedral design principle. *Nat. Commun.* **2019**, *10*, 4414. [CrossRef]
21. Sharma, M.; Biela, A.P.; Kowalczyk, A.; Borzecka-Solarz, K.; Piette, B.M.; Gaweł, S.; Bishop, J.; Kukura, P.; Benesch, J.L.; Imamura, M.; et al. Shape-morphing of an artificial protein cage with unusual geometry induced by a single amino acid change. *ACS Nanosci. Au* **2022**, *2*, 404–413. [CrossRef] [PubMed]
22. McTernan, C.T.; Davies, J.A.; Nitschke, J.R. Beyond Platonic: How to Build Metal-Organic Polyhedra Capable of Binding Low-Symmetry, Information-Rich Molecular Cargoes. *Chem. Rev.* **2022**, *122*, 10393–10437. [CrossRef]
23. Khmelinskaia, A.; Wargacki, A.; King, N.P. Structure-based design of novel polyhedral protein nanomaterials. *Curr. Opin. Microbiol.* **2021**, *61*, 51–57. [CrossRef] [PubMed]

24. Laniado, J.; Yeates, T.O. A complete rule set for designing symmetry combination materials from protein molecules. *Proc. Natl. Acad. Sci. USA* **2020**, *117*, 31817–31823. [CrossRef]

25. Stupka, I.; Biela, A.P.; Piette, B.; Kowalczyk, A.; Majsterkiewicz, K.; Borzęcka-Solarz, K.; Naskalska, A.; Heddle, J.G. An Artificial Protein Cage Made from a 12-Membered Ring. *J. Mater. Chem.* **2024**, *12*, 436–447. [CrossRef] [PubMed]

26. Kirkpatrick, S.; Gelatt, C.D., Jr.; Vecchi, M.P. Optimization by Simulated Annealing. *Science* **1983**, *220*, 671–680. [CrossRef]